JOURNAL OF COMPUTATIONAL PHYSICS 122, 335–342 (1995)

Momentum Lattice Simulation on a Small Lattice Using Stochastic Quantization

H. KRÖGER AND S. LANTAGNE

Département de Physique, Université Laval, Québec, Québec G1K 7P4, Canada

AND

K. J. M. MORIARTY

Department of Mathematics, Statistics and Computing Science, Dalhousie University, Halifax, Nova Scotia B3H 3J5, Canada

Received November 17, 1994; revised April 25, 1995

We have studied the scalar ϕ^4-model in the symmetric phase near the phase transition and the non-compact $U(1)$ gauge theory on a momentum lattice using the Langevin equation for generating configurations. In the ϕ^4-model we have computed the renormalized mass and in the $U(1)$-model we have computed the Wilson loop operator. We used a second-order algorithm for solving the Langevin equation, and we studied the convergence rate of the method. We looked at the stochastic time needed to generate equilibrium configurations and compared first- and second-order schemes for both models.

1. INTRODUCTION

One major problem in lattice gauge theory has been the increased amount of computer time and memory needed to do simulations near a critical point. The so-called critical slowing down can be countered, e.g., with the Fourier acceleration method [1]. Other methods have been developed, e.g., the cluster algorithm [2], which is very successful to accelerate convergence at the critical point for Ising-type systems. When we studied the scalar ϕ^4-model near the critical point on a *momentum lattice* [3], it turned out that quite reasonable results for the renomalized mass, wave function renormalization, etc., could be obtained on relatively small lattices (3^4–7^4). In this note we want to report a more detailed numerical analysis of the convergence behavior on a momentum lattice.

2. MOMENTUM SPACE

Momentum space has several interesting advantages over coordinate space:

- The kinetic energy of the action is local.
- One can implement Fourier acceleration to fight critical slowing down.
- At the critical point, the correlation length goes to infinity. The behavior at $x \to \infty$ in coordinate space corresponds to $k \to 0$ in momentum space.
- The correlation function in momentum space behaves as $1/(m_R^2 + k^2)$ near the critical point. At the critical point, $m_R \to 0$, but one can stay away from the pole by choosing some $k^2 \neq 0$.
- Although the action in momentum space is non-local, one can use a fast Fourier transform to switch to coordinate space, where the interaction is local.

3. STOCHASTIC QUANTIZATION

We have used stochastic quantization, which is a practical method to go from the continuum formulation to algorithms for numerical simulations. We have studied the ϕ^4_{3+1} model and the non-compact $U(1)_{3+1}$ gauge model. Stochastic quantization was introduced by Parisi and Wu [4], and it has been applied by many authors (for a review see Damgaard and Hüffel [5, 6]). The idea is to consider the Euclidean quantum field as the equilibrium state of a statistical system coupled to a heat reservoir. Parisi and Wu have introduced a fifth coordinate τ, called stochastic (fictious) time. The evolution of this statistical system in stochastic time is described by a Langevin equation. To be more specific, let us consider the scalar ϕ^4_{3+1} model in its Euclidean form. Its action reads

$$S_E = \int d^4x \frac{1}{2} \partial_\mu \phi(x) \partial_\mu \phi(x) + \frac{m^2}{2} \phi^2(x) + \frac{g}{4!} \phi^4(x). \qquad (1)$$

The Langevin equation, governing the evolution reads

$$\frac{\partial \phi(x, \tau)}{\partial \tau} = - \frac{\delta S[\phi]}{\delta \phi(x)} \Big|_{\phi(x)=\phi(x,\tau)} + \eta(x, \tau). \qquad (2)$$

Here $\eta(x, \tau)$ is a field of Gaussian noise obeying

0021-9991/95 $12.00

$$\langle \eta(x, \tau) \rangle_\eta = 0,$$
$$\langle \eta(x', \tau')\eta(x, \tau) \rangle_\eta = 2\delta(x - x')\delta(\tau' - \tau). \quad (3)$$

The average $\langle \, \rangle_\eta$ is defined by a functional integral over the noise with a Gaussian distribution

$$\langle O[\eta] \rangle_\eta = \frac{\int D\eta \, O[\eta] \exp[-\frac{1}{4} \int d^4x \, d\tau \, \eta^2(x, \tau)]}{\int D\eta \exp[-\frac{1}{4} \int d^4x \, d\tau \, \eta^2(x, \tau)]}. \quad (4)$$

Our goal is to solve the Langevin equation many times to generate a good representation of the statistical ensemble. This generates the field $\phi[\eta]$ as a functional of the noise η. In order to obtain the vacuum expectation value of a physical observable one performs the average of the desired observable, according to Eq. (4). The relation between stochastic quantization and quantization by functional integrals is expressed by the following central result of stochastic quantization: When $\tau \to \infty$ the statistical system is "equal" to the Euclidean field; i.e., the stochastic n-point correlation function coincides with the Euclidean n-point correlation function

$$\lim_{\tau\to\infty} \langle \phi(x_1, \tau)[\eta] \cdots \phi(x_n, \tau)[\eta] \rangle_\eta = \langle \phi(x_1) \cdots \phi(x_n) \rangle_E. \quad (5)$$

4. MOMENTUM SPACE AND LATTICE REGULARIZATION

Via a Fourier transformation

$$\hat{\phi}(k, \tau) = \int \frac{d^4k}{(2\pi)^4} \exp[-ikx]\phi(x, \tau), \quad (6)$$

the action (1) is transformed into momentum space

$$S = \frac{1}{2} \int \frac{d^4k}{(2\pi)^4} (k^2 + m^2)\hat{\phi}(k)\hat{\phi}(-k)$$
$$+ \frac{g}{4!} \int \frac{d^4k}{(2\pi)^4} \frac{d^4p}{(2\pi)^4} \frac{d^4q}{(2\pi)^4} \hat{\phi}(k)\hat{\phi}(p)\hat{\phi}(q)\hat{\phi}(-k - p - q). \quad (7)$$

The Langevin equation corresponding to Eq. (2) reads in momentum space

$$\frac{\partial \hat{\phi}(k, \tau)}{\partial \tau} = -(2\pi)^4 \frac{\delta S[\hat{\phi}]}{\delta \hat{\phi}(-k)} \Big|_{\hat{\phi}(-k) = \hat{\phi}(-k,\tau)} + \hat{\eta}(k, \tau). \quad (8)$$

Here $\hat{\eta}(k, \tau)$ is the field of Gaussian noise obeying

$$\langle \hat{\eta}(k, \tau) \rangle_\eta = 0,$$
$$\langle \hat{\eta}(k', \tau')\hat{\eta}(k, \tau) \rangle_\eta = 2(2\pi)^4\delta(k' + k)\delta(\tau' - \tau). \quad (9)$$

We regularize the field theory by introducing a momentum lattice, being a regular hypercube in four dimensions. It is characterized by a resolution Δk and an ultraviolet cutoff Λ. Lattice sites are denoted by k_I. The action on the momentum lattice is obtained from Eq. (7). Note that the original noise field has a delta function normalization with respect to coordinates and stochastic time. In order to solve the Langevin equation numerically, one has to discretize also the stochastic time τ, by introducing a step size $\Delta\tau$. Then in order to normalize the noise to a Kronecker delta function, one introduces the rescaled field and noise

$$\tilde{\phi}(k_I, \tau_a) = \left(\frac{\Delta k}{2\pi}\right)^2 \hat{\phi}(k_I, \tau_a),$$
$$\tilde{\eta}(k_I, \tau_a) = (\Delta\tau)^{1/2} \left(\frac{\Delta k}{2\pi}\right)^2 \hat{\eta}(k_I, \tau_a). \quad (10)$$

The noise obeys now

$$\langle \tilde{\eta}(k_I, \tau_a)\tilde{\eta}(k_J, \tau_b) \rangle = 2\delta_{k_I+k_J,0}\delta_{\tau_a,\tau_b}. \quad (11)$$

Thus the Langevin equation (8) can be written as a first-order iterative scheme

$$\tilde{\phi}(k_I, \tau_a + \Delta\tau) = (1 - \Delta\tau(k_I^2 + m^2))\tilde{\phi}(k_I, \tau_a)$$
$$- \Delta\tau \frac{g}{3!} \sum_{k_J, k_M} \left(\frac{\Delta k}{2\pi}\right)^4 \tilde{\phi}(k_J, \tau_a)\tilde{\phi}(k_M, \tau_a)\,\tilde{\phi}(k_I - k_J - k_M, \tau_a)$$
$$+ \sqrt{\Delta\tau}\,\tilde{\eta}(k_I, \tau_a). \quad (12)$$

In a similar way one can set up a second-order scheme (second-order Runge–Kutta). This equation has to be solved for a large number of configurations of noise. Finally, one has to take the average over the statistical ensemble. The expectation value of an observable is defined by

$$\overline{O[\hat{\phi}]} = \lim_{T\to\infty} \frac{1}{T} \int_0^T d\tau' \, O[\hat{\phi}(\tau')]. \quad (13)$$

Because we suppose that our system is ergodic, the expectation value can be computed by summing over the configurations,

$$\langle O[\hat{\phi}] \rangle = \lim_{N\to\infty} \frac{1}{N} \sum_{n=1}^{N} O[\hat{\phi}_n]. \quad (14)$$

Let N denote the size of the statistical ensemble, i.e., the number of throwing a dice but with Gaussian distribution for each lattice momentum k_I, i.e., the number of configurations of noise. One must solve the Langevin equation N times in parallel, which can be done using a parallel processor. This yields the field $\hat{\phi}$ being a functional of the noise $\hat{\eta}$. Then one computes the expectation of an observable by taking the average over the statistical ensemble, i.e., by summing over the field configurations. The number of configurations of noise, which have been used in the numerical simulations varies between $N = 301{,}420$ for the ϕ^4 model on the 3^4 lattice and $N = 256$ for the $U(1)$ model for the Wilson loop (see details below).

5. NUMERICAL ASPECTS

The momentum lattice and the Langevin algorithm is characterized by the following set of parameters:

(a) Size of lattice L^4 ($L \to \infty$).

(b) Lattice resolution Δk and ultra violet lattice cutoff Λ ($2\Lambda = (L-1)\Delta k$), ($\Delta k \to 0$, $\Lambda \to \infty$).

(c) Order of scheme to solve stochastic differential equation.

(d) Step size $\Delta\tau$ ($\Delta\tau \to 0$).

(e) Finite upper limit τ_{final}, ($\tau_{\text{final}} \to \infty$).

(f) Size of statistical ensemble, i.e., the number N of configurations of noise ($N \to \infty$).

We have indicated in parenthesis to which limit these parameters should tend in the continuum limit of the theory.

In a numerical simulation, one has to test stability of the results with respect to variation of those parameters. The Langevin equation is a first-order differential equation that we integrate up to a final value τ_{final}, by increments of $\Delta\tau$. The need to choose a large value for τ_{final} can be seen from the free scalar model (obtained by putting $g = 0$ in the action, Eq. (1)). The Euclidean Feynman propagator (two-point function) for the free scalar theory reads

$$\langle \hat{\phi}(k)\hat{\phi}(k')\rangle = (2\pi)^4\, \delta(k+k')\, \frac{1}{k^2+m^2}. \qquad (15)$$

The Euclidean propagator in stochastic quantization with continuous stochastic time τ is given by [6]

$$\begin{aligned}\langle \hat{\phi}(k,\tau)\hat{\phi}(k',\tau')\rangle = (2\pi)^4 \frac{\delta(k+')}{k^2+m^2} \\ \times [\exp\{-|\tau-\tau'|(k^2+m^2)\} \qquad (16) \\ -\exp\{-(\tau+\tau')(k^2+m^2)\}].\end{aligned}$$

We can see that one must choose $\tau = \tau' = \tau_{\text{final}}$ and $\tau_{\text{final}}(k^2 + m^2))$ must be large enough to make the second exponential term negligible. It should be noted that this corresponds to a solution of the Langevin equation with the boundary condition $\tilde{\phi}(k, \tau = 0) = 0$. Other boundary conditions may give different results for finite τ, τ', but will give the same result in the limit $\tau = \tau' \to \infty$.

This holds for the case of continuous momenta and stochastic time. There is no need to introduce a finite $\Delta\tau$. However, when we consider the ϕ^4 model on the momentum lattice and discretize stochastic time, we have to introduce a finite $\Delta\tau$ and we have to choose it to be small. It turns out that one cannot vary both τ_{final} and $\Delta\tau$ independently. This can be seen as follows: Again we look at the free scalar model, on the momentum lattice with discrete stochastic time, corresponding to the Langevin Eq. (12) with $g = 0$,

$$\frac{\Delta}{\Delta\tau}\tilde{\phi}(\tau_a) = -A\tilde{\phi}(\tau_a) + (\Delta\tau)^{-1/2}\tilde{\eta}(\tau_a). \qquad (17)$$

Here $\Delta/\Delta\tau$ stands for the finite difference operator and $A(k) = k^2 + m^2$. Let us suppress the k-dependence for the moment. In particular we are interested in the solution with the boundary condition

$$\tilde{\phi}(\tau_a = 0) = 0. \qquad (18)$$

The Green's function $\tilde{G}$ is defined as the solution of

$$\frac{\Delta}{\Delta\tau}\tilde{G}(\tau_a) = -A\tilde{G}(\tau_a) + \delta_{\tau_a,0}. \qquad (19)$$

Then the general solution of Eq. (17) can be expressed as

$$\begin{aligned}\tilde{\phi}(\tau_a) = \sum_{\tau_b} [\tilde{G}(\tau_a - \tau_b) - \tilde{G}(-\tau_b)\hat{\phi}^{\text{hom}}(\tau_a)](\Delta\tau)^{-1/2}\tilde{\eta}(\tau_b) \qquad (20) \\ + \text{const} \times \tilde{\phi}^{\text{hom}}(\tau_a),\end{aligned}$$

where $\tilde{\phi}^{\text{hom}}$ satisfies the homogeneous equation corresponding to Eq. (17). The Green's function can be computed via a discrete Fourier transformation

$$f(\tau_a) = \sum_{\sigma_a} \frac{\Delta\sigma}{2\pi}\exp[i\tau_a\sigma_a]\bar{f}(\sigma_a) \qquad (21)$$

and yields

$$\tilde{G}(\tau_a) = \sum_{\sigma_b} \frac{\Delta\sigma}{2\pi}\exp[i\tau_a\sigma_b]\left(\Delta\tau\Big/\left(A + i\frac{\sin(\Delta\tau\sigma_b)}{\Delta\tau}\right)\right). \qquad (22)$$

The solution of the homogeneous equation in continuous stochastic time reads $\hat{\phi}^{\text{hom}}(\tau) = \exp[-A\tau]$, which corresponds to the boundary condition $\hat{\phi}^{\text{hom}}(\tau = 0) = 1$. Then the homogeneous solution in discrete stochastic time can be expressed as

$$\tilde{\phi}^{\text{hom}}(\tau_a) = \exp[-A\tau_a][1 + O(\Delta\tau)]. \qquad (23)$$

Now we can compute the two-point function (propagator) corresponding to the boundary condition (18), which requires const $= 0$ in Eq. (20),

$$\langle\tilde{\phi}(k_I, \tau_a)\tilde{\phi}(k_J, \tau_b)\rangle = 2\,\delta_{k_I+k_J,0}\,(\Delta\tau)^{-1} \times \sum_{\tau_m} [\tilde{G}(k_I, \tau_a - \tau_m) - \tilde{G}(k_I, -\tau_m)\tilde{\phi}^{\text{hom}}(k_I, \tau_a)] \times [\tilde{G}(-k_I, \tau_b - \tau_m) - \tilde{G}(-k_I, -\tau_m)\tilde{\phi}^{\text{hom}}(-k_I, \tau_b)]. \quad (24)$$

There are four terms in the square brackets, yielding

$$\langle\tilde{\phi}(k_I, \tau_a)\tilde{\phi}(k_J, \tau_b)\rangle = 2\,\delta_{k_I+k_J,0} \sum_{\sigma_p} \frac{\Delta\sigma}{2\pi} \times \left[\frac{\exp[i(\tau_a - \tau_b)\sigma_p]}{(m^2 + k_I^2)^2 + \sin^2(\Delta\tau\sigma_p)/\Delta\tau^2} - \frac{\exp[i\tau_a\sigma_p]}{(m^2 + k_I^2)^2 + \sin^2(\Delta\tau\sigma_p)/\Delta\tau^2}\tilde{\phi}^{\text{hom}}(-k_I, \tau_b) - \frac{\exp[-i\tau_a\sigma_p]}{(m^2 + k_I^2)^2 + \sin^2(\Delta\tau\sigma_p)/\Delta\tau^2}\tilde{\phi}^{\text{hom}}(k_I, \tau_a) + \frac{1}{(m^2 + k_I^2)^2 + \sin^2(\Delta\tau\sigma_p)/\Delta\tau^2}\tilde{\phi}^{\text{hom}}(k_I, \tau_a)\tilde{\phi}^{\text{hom}}(-k_I, \tau_b)\right]. \quad (25)$$

Now we can see what happens when we approach the continuum limit in Eq. (25): When we first go to the limit $\Delta\tau \to 0$, $\Delta\sigma \to 0$, and evaluate the integrals via the residue theorem, we obtain the expression given by Eq. (16). Then taking the limit $\tau_a = \tau_b = \tau_{\text{final}} \to \infty$, and finally let $\Delta k \to 0$, we obtain the continuum result for the propagator, given by Eq. (15). If, however, we keep $\Delta\tau$ fixed and let $\tau_a, \tau_b \to \infty$, then the propagator starts to oscillate after a while due to the presence of the sin term in the denominator of Eq. (25). Thus we expect the following behavior of correlation functions as a fucntion of τ_{final} and $\Delta\tau$ (the parameter $1/m$ can be chosen to set the scale for τ): For fixed $\Delta\tau$, the correlation function varies strongly for small τ_{final}, then reaches a region of small variation (plateau region) and then starts to oscillate for large τ_{final}. For another smaller value of $\Delta\tau$, one expects a wider size of the plateau region. This behavior is actually seen in the numerical data: First, we show in Figs. 2a, b, c the renormalalized mass of the ϕ^4 model as a function of τ_{final}. We have varied $\Delta\tau$: $\Delta\tau = 1.0$, 0.5, 0.25. We have compared a first order with a second-order algorithm. The latter uses the interval $\Delta\tau/2$ to estimate the functional increment compared to the former which uses the interval $\Delta\tau$. For $\Delta\tau = 1.0$, we observe fluctuations when varying τ_{final}. When going to $\Delta\tau = 0.5$ and $\Delta\tau = 0.25$, the fluctuations disappear and a plateau region is formed. Second, we show in Figs. 4 and 5 the Wilson loop for the $U(1)$ model. The difference between the two figures is just the value of $\Delta\tau$: The value corresponding to Fig. 5 is smaller by a factor 1.5 then the value corresponding to Fig. 4. The data of Fig. 5 show a better agreement with the analytical results than those of Fig. 4.

Before discussing in more detail the numerical results, let us define the physical observables which we have computed in the ϕ^4 model: The renormalized mass m_R and the wave function renormalization Z_R are defined via the connected 2-point function (after splitting off the factor $(2\pi)^4\delta(k_{\text{total}})$),

$$G^{(2)}_{\text{conn}}(k) = \langle\hat{\phi}(k)\hat{\phi}(-k)\rangle_{\text{conn}} = \frac{Z_R}{m_R^2 + k^2 + O(k^4)}. \quad (26)$$

The values of m_R and Z_R have been extracted by doing a quartic fit of the inverse propagator

$$[G^{(2)}_{\text{conn}}(k)]^{-1} = A + Bk^2 + Ck^4. \quad (27)$$

Finally, in order to compare our results with Lüscher and Weisz' results [7], we have reparametrized the bare parameters m, g of the action and rescaled the field ϕ, in terms of κ, λ, and ϕ_0,

$$\phi_0(x) = \sqrt{2\kappa}\phi(x), \quad m^2 = (1 - 2\lambda)/\kappa - 8, \quad g = 6\lambda/\kappa^2. \quad (28)$$

Lüscher and Weisz have studied the ϕ^4 model in the symmetrical phase close to the phase transition and computed the renormalized coupling constant, renormalized mass, and wave function renormalization. They have used the hopping parameter expansion up to 14th order (expansion of the functional integral on the space time lattice in terms of the kinetic term), which allowed them to approach $\kappa \to \kappa_{\text{crit}}$ by 95%. Then they used renormalization group equations to extrapolate this to the critical line.

The Langevin equation can be solved using a standard method like Euler's method where the truncation term is $O(\Delta\tau^2)$, or a higher order scheme like Heun's method (second-order Runge–Kutta), where the truncation term is $O(\Delta\tau^3)$. Batrouni *et al.* [1] have shown that a higher order integration scheme has many advantages, and our experience [3] agrees with theirs. For the same level of error, Heun's method is faster; it takes fewer stochastic time steps. For the same stochastic time step, it was 46% slower for the ϕ^4-model, but in the case of the non-compact $U(1)$-model it was only 12% slower; in the case of the ϕ^4-model, the second-order scheme required the evaluation of two additional fast Fourier transforms, but in the case of the $U(1)$-model only a few more additions and multiplications were required. In Fig. 1 we display for the ϕ^4-model the behavior of the renormalized mass m_R in the neighborhood of the critical point and compare it to the results obtained by Lüscher and Weisz. Our results correspond to a 3^4 lattice, where we have used $N = 301{,}420$ configurations of Gaussian noise and to a 7^4 lattice, where we have used $N = 17{,}920$ configurations of noise. We have used the parameter $\lambda = 0.00345739$, Eq. (28), and the lattice spacing $\Delta k = 1$. We want to point out that we are quite close to the critical line, the renormalized mass m_R

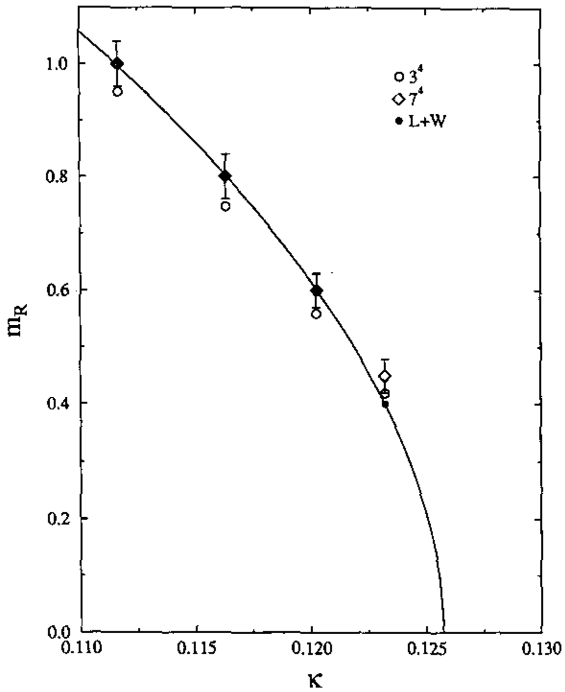

FIG. 1. Renormalized mass m_R of the ϕ^4-model versus coupling parameter κ. The semi-analytical results are taken from Lüscher and Weisz, Ref. [7]. The full curve is a fit to Lüscher and Weisz's results using the scaling behavior predicted by the renormalisation group at the critical point [7].

is quite small, and, hence, the two-point function is strongly dominated by small momenta.

We have plotted in Figs. 2a, b, c the renormalized mass m_R as a function of τ_{final} for different values of $\Delta\tau$ computed on a lattice of 3^4 points. We have used $N = 1024$ configurations of noise. The calculation corresponds to a coupling parameter $\kappa = 0.12025$, while the critical point is at $\kappa_c = 0.1257(1)$. The parameters λ and Δk are as in Fig. 1. The results corresponding to $\Delta\tau = 1.0$ are shown in Fig. 2a. There are fluctuations for all values of τ_{final}. When going to $\Delta\tau = 0.5$ (Fig. 2b), one observes a region of stability $15 \leq \tau_{\text{final}} \leq 25$ being formed, and fluctuations are seen for $\tau_{\text{final}} \geq 25$. However, these fluctuations are less pronounced than those corresponding to $\Delta\tau = 1.0$. Finally, the results corresponding to $\Delta\tau = 0.25$ are shown in Fig. 2c. One observes a region of stability $22 \leq \tau_{\text{final}} \leq 32$, and the fluctuations are smaller than in the previous two cases. Also, one observes the results corresponding to the first-order algorithm approaching those of the second-order algorithm, when $\Delta\tau$ becomes smaller.

6. NON-COMPACT $U(1)$ GAUGE THEORY

The Euclidean action for non-compact $U(1)$ gauge theory is given by

$$S = \frac{1}{4}\int d^4x F_{\mu\nu}(x) F_{\mu\nu}(x), \qquad (29)$$

where

$$F_{\mu\nu}(x) = \partial_\mu A_\nu(x) - \partial_\nu A_\mu(x) \qquad (30)$$

is the field strength tensor and A_μ is the gauge field. In momentum space the action takes the form

$$\begin{aligned} S &= \frac{1}{4}\int \frac{d^4k}{(2\pi)^4} \hat{F}_{\mu\nu}(k)\hat{F}_{\mu\nu}(-k), \\ &= \frac{1}{2}\int \frac{d^4k}{(2\pi)^4} \hat{A}_\mu(k) k^2 T_{\mu\nu}(k) \hat{A}_\nu(-k), \end{aligned} \qquad (31)$$

where

$$T_{\mu\nu}(k) = \delta_{\mu\nu} - (k_\mu k_\nu)/k^2 \qquad (32)$$

is a projector on the transverse gauge field. This model of non-interacting non-compact gauge theory is analytically solvable. Thus this model can serve as a numerical test of the stochastic quantization method for a gauge theory. The action, Eq. (29), is invariant under local $U(1)$ gauge transformations. Let us recall what happens with gauge symmetry in the stochastic quantization method [4, 5]. In path integral quantization, using perturbation theory, one has to fix the gauge. Non-perturbatively, a gauge fixing condition is in general not unique, which leads to the so-called Gribov ambiguity problem. In stochastic quantization, gauge fixing is not necessary and, hence, avoids the Gribov problem, which was one of the incentives by Parisi and Wu [4]. One finds that gauge dependent quantities, like the photon propagator of the Maxwell field (see Eq. (33)), diverge when $\tau \to \infty$. One the other hand, gauge independent observables, like the field tensor or its correlation function (see Eq. (34)) are free of such divergence and tend to the usual answer, when $\tau \to \infty$. One obtains for the two-point function

$$\begin{aligned} \langle \hat{A}_\mu(k,\tau)\hat{A}_\nu(k',\tau)\rangle &= (2\pi)^4\delta(k+k') \\ &\left[T_{\mu\nu}\frac{1}{k^2}(1-\exp(-2k^2\tau)) + 2L_{\mu\nu}\tau\right], \end{aligned} \qquad (33)$$

where $L_{\mu\nu} = \delta_{\mu\nu} - T_{\mu\nu}$ is the projector on the longitudinal gauge field. That implies for the correlation function of the field tensor

$$\begin{aligned} &\langle F_{\mu\nu}(k,\tau)\hat{F}_{\sigma\rho}(k',\tau)\rangle \\ &\quad = (2\pi)^4\delta(k+k')(1-\exp(-2k^2\tau))\frac{1}{k^2} \\ &\quad \times \{k_\mu k_\sigma \delta_{\nu\rho} - k_\nu k_\sigma \delta_{\mu\rho} - k_\mu k_\rho \delta_{\nu\sigma} + k_\nu k_\rho \delta_{\mu\sigma}\} \end{aligned} \qquad (34)$$

and, hence,

$$\lim_{\tau\to\infty}\langle \hat{F}_{\mu\nu}(k,\tau)\hat{F}_{\mu\nu}(k',\tau)\rangle = 6(2\pi)^4\delta(k+k'). \qquad (35)$$

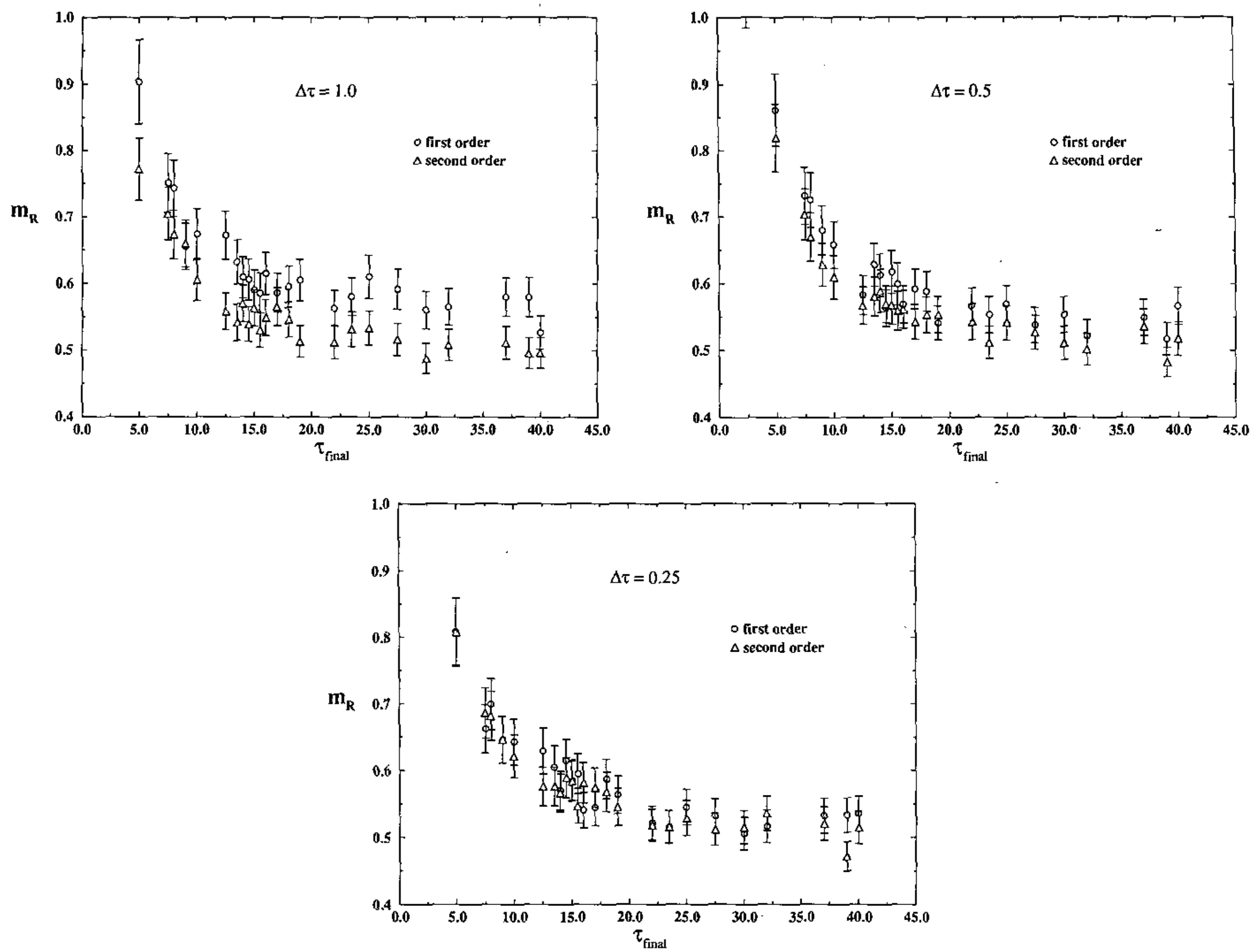

FIG. 2. (a) Renormalized mass m_R of the ϕ^4-model versus stochastic time τ_{final}. $\Delta\tau = 1.0$. (b) Same as (a), but $\Delta\tau = 0.5$. (c) Same as (a), but $\Delta\tau = 0.25$.

This gauge theory can be discretized on a momentum lattice like the scalar ϕ^4 theory. The action reads

$$\begin{aligned} S &= \frac{1}{4}\sum_{k_l}\left(\frac{\Delta k}{2\pi}\right)^4 \hat{F}_{\mu\nu}(k_l)\hat{F}_{\mu\nu}(-k_l) \\ &= \frac{1}{2}\sum_{k_l}\left(\frac{\Delta k}{2\pi}\right)^4 \hat{A}_\mu(k_l)k_l^2 T_{\mu\nu}(k_l)\hat{A}_\nu(-k_l). \end{aligned} \tag{36}$$

What happens with gauge symmetry? The non-compact $U(1)$ gauge theory can be formulated on a standard space–time lattice, such that gauge symmetry is manifestly conserved on a finite lattice. We define a local gauge transformation on the momentum lattice by

$$\hat{A}_\mu(k_l) \rightarrow \hat{A}'_\mu(k_l) = \hat{A}_\mu(k_l) + (k_l)_\mu \hat{\chi}(k_l). \tag{37}$$

Then the field tensor $\hat{F}_{\mu\nu}(k_l)$ and the action, Eq. (36), are invariant under this transformation.

We have done a numerical simulation via stochastic quantization on the momentum lattice. We have evaluated the expectation value $\langle F_{\mu\nu}F_{\mu\nu}\rangle$. We have used $\Delta k = 2\pi/La$ as lattice spacing, where $a = 1$ the lattice spacing of the space-time lattice and L is the number of sites in each dimension. In Fig. 3 we show $\langle F_{\mu\nu}F_{\mu\nu}\rangle$ versus the number N of configurations of noise. The error shows a typical $1/\sqrt{N}$ behavior. The numerical results differ from the analytical result by about 1%. The remaining error is due to finite $\Delta\tau$ and finite τ_{final}. It should be noted that $\langle F_{\mu\nu}F_{\mu\nu}\rangle$ is a local observable in momentum space.

Numerically more challenging is the determination of a non-local observable, like the Wilson loop. For a given oriented closed curve C, the Wilson loop along the curve C is defined via

$$W_P = \exp\left[ig\int_C dx_\mu A^\mu(x)\right]. \tag{38}$$

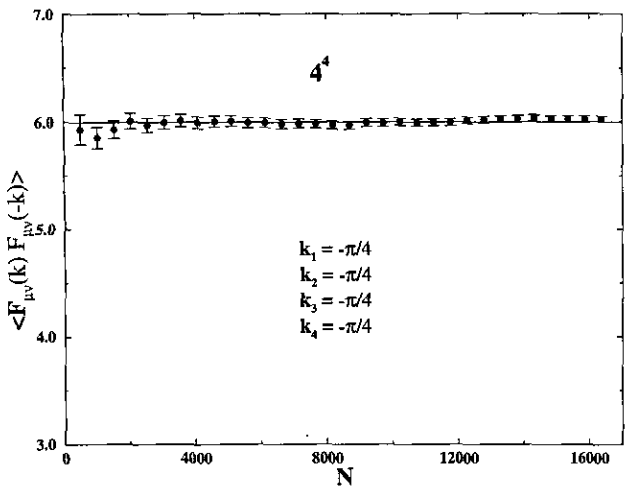

FIG. 3. $U(1)$-model. Expectation value $\langle F_{\mu\nu}(k)\, F_{\mu\nu}(-k)\rangle$ versus size of ensemble of Gaussian noise. Full line: analytical result, Eq. (35).

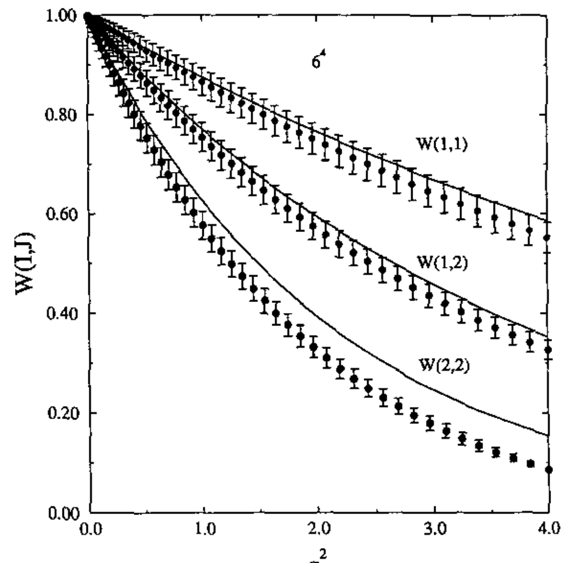

FIG. 4. $U(1)$-model. Wilson loop $W(I, J)$ versus coupling constant g; $\Delta\tau = \tau_{\text{final}}/100$. Full line: analytical result, Eq. (39).

In quantum chromodynamics (QCD), the standard theory of strong interactions, the Wilson loop corresponds to the creation of a quark–antiquark pair, the propagation of this "meson" and the destruction of the quark–antiquark pair. It plays the role of an order parameter for confinement. For the $U(1)$ theory the Wilson loop can be computed analytically. Let the curve C be given by a rectangle of size $R \times T$, being located in a two-dimensional plane. Then the Euclidean Wilson loop expressed in momentum space can be written

$$\langle W_P\rangle = \exp\left[\frac{-g^2}{2}\int_{-\Lambda}^{\Lambda}\frac{d^4k}{(2\pi)^4}\,\frac{k_1^2+k_2^2}{k^2}\left(\frac{2\sin(k_1R/2)}{k_1}\right)^2 \cdot \left(\frac{2\sin(k_2T/2)}{k_2}\right)^2\right]. \tag{39}$$

Here Λ denotes a high momentum cutoff, necessary to regularize the otherwise divergent integral.

We have chosen to simulate the Wilson loop being a non-local observable because it should be a more stringent test than $\langle F_{\mu\nu}F_{\mu\nu}\rangle$. Second, the g dependence of W_P (Eq. (38)) means a more rapidly oscillating function for large g. From this we expect that the larger g is, the more difficult will it be to obtain agreement between numerical and analytical results. We considered $W_P(I, J)$, where $I \times J$ denotes the size of the rectangular loop measured in units of the lattice spacing. Note that the gauge field configurations generated by the action are independent from the coupling parameter g, which appears in the observable W_P. Consequently different size Wilson loops and Wilson loops for different values of g all correspond to the same gauge field configurations, only the observables differ. In this sense the statistical errors are correlated. The Wilson loop seems to be more sensitive than $\langle F_{\mu\nu}F_{\mu\nu}\rangle$. When integrating the Langevin equation, if we integrate beyond the region of stability, then fluctuations occur in the solution. These fluctuations are more important for non-local observables. In Figs. 4 and 5, we show the expectation value of the Wilson loop operator for different loop sizes and for different stochastic time steps. The lattice size is 6^4. The number of configurations of noise is $N = 256$. In order to equilibrate the error due to finite τ_{final} (see Eq. (33)) we have chosen τ_{final} depending on the lattice momentum: $\tau_{\text{final}} = 10/k_l^2$. For a given value value of τ_{final}, Fig. 4 corresponds to $\Delta\tau = \tau_{\text{final}}/100$, while Fig. 5 corresponds to $\Delta\tau = \tau_{\text{final}}/150$. The lattice spacing Δk is as in Fig. 3. We have

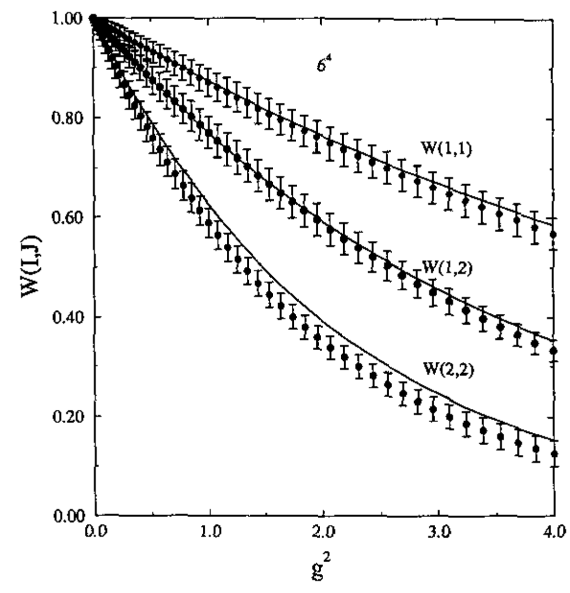

FIG. 5. Same as Fig. 4, but $\Delta\tau = \tau_{\text{final}}/150$.

also plotted the result of the analytic expression (39). We make the following observations:

(a) The lattice size (6^4) limits the size of the loops, which can be measured in a meaningful way. As a general rule, the loop size should not exceed half of the lattice size. Both, Figs. 4 and 5 show that the smaller the loop (the smallest one being $W_P(1, 1)$), the better is the agreement with the analytic expression. This is a typical finite size effect of the lattice.

(b) Both, Figs. 4 and 5 also show that the smaller the value of g, the better is the agreement with the analytic expression. Larger values of g correspond to an observable W_P with more rapid oscillations as a function of momentum. As can be seen from Eq. (39), important contributions to W_P come from the region around $k = 0$. Thus the origin of these discrepancies should be effects due to finite lattice resolution Δk.

(c) Comparing Figs. 4 and 5, we observe that the simulation with smaller $\Delta\tau$ gives results closer to the analytic expression. This is in agreement with the behavior discussed for the scalar ϕ^4 theory in Secion 5.

7. CONCLUSION

Our study of the scalar ϕ^4_{3+1} theory and the $U(1)_{3+1}$ gauge theory shows the feasibility of doing lattice simulations on a small momentum lattice. The second-order scheme turned out to be by far more appropriate because of its greater accuracy and speed. For both, the propagator of the ϕ^4 model near the critical point, where the renormalized mass goes to zero, as well for the Wilson loop in $U(1)$ model, the small momentum behavior ($k \approx 0$) plays an important role. For the ϕ^4 theory we have identified a region of stability (plateau) in the stochastic time parameter τ_{final}. We have studied the stability of the results under variation of $\Delta\tau$ in the simulation of the scalar ϕ^4 theory and for the Wilson loop in the $U(1)$ gauge theory. The knowledge of the stability region is very important for simulations of theories like $SU(2)$ and $SU(3)$. For these models, the time needed for generating equlibrium configurations is much larger than for the $U(1)$-model. How about the usefulness of the momentum lattice regularization and the efficiency of Langevin updating on a momentum lattice? We have given two examples, where the small momentum behavior plays an important role for physics: the propagator of a massive model near the critical point and, second, the Wilson loop for a massless model. It turns out for the scalar model that the critical behavior can be obtained quite well on a small momentum lattice. The disadvantage of updating on a momentum lattice compared to a space–time lattice is the property of a non-local action, which makes each update more costly in computing time. The most efficient way of doing the updating is by going via fast Fourier transform to space—time, doing the updating using the locality of the action and then going back by fast Fourier transform. Thus the effort for updating goes like $V \log V$ on the momentum lattice compared to V on a space–time lattice (V being the lattice volume).

ACKNOWLEDGMENT

H.K. wants to acknowledge support by NSERC Canada.

REFERENCES

1. G. G. Batrouni, G. R. Katz, A. S. Kronfeld, G. P. Lepage, B. Svetitsky, and K. G. Wilson, *Phys. Rev. D* **32,** 2736 (1985).
2. R. H. Swendsen and J. S. Wang, *Phys. Rev. Lett.* **58,** 86 (1987).
3. D. Bérubé, H. Kröger, R. Lafrance, and S. Lantagne, *Phys. Rev. D* **44,** 2604 (1991).
4. G. Parisi and Y. Wu, *Sci. Sin.* **24,** 483 (1981).
5. P. H. Damgaard and H. Hüffel, *Stochastic Quantization* (World Scientific, Singapore, 1988).
6. P. H. Damgaard and H. Hüffel, *Phys. Rep.* **152,** 227 (1987).
7. M. Lüscher and P. Weisz, *Nucl. Phys. B* **290,** 25 [FS20] (1987).
8. G. Bhanot and M. Creutz, *Phys. Rev. D* **21,** 2892 (1980); M. Creutz, *Phys. Rev. D* **23,** 1815 (1981).